INNOVATIVE MECHANICAL ENGINEERING **ISSN 2812-9229 (Online)**
University of Niš, Faculty of Mechanical Engineering
VOL. 1, NO 2, 2022, PP. 01 - 10

Original scientific paper *

FEM ANALYSIS OF THE DEEP DRAWING PROCESS

Saša Ranđelović[1], Mladomir Milutinović[2], Marina Trajković[3],

Dejan Movrin[2], Nikola Kostić[4]

[1]University of Niš, Faculty of Mechanical Engineering

[2]University of Novi Sad, Faculty of Technical Sciences

[3]University of Niš, Faculty of Civil Engineering and Architecture

[4]Academy of Technical Educational Vocational Studies Niš

Abstract. *The deep drawing process is a metal forming technology that requires the analysis of several influencing factors. Its finite element simulation is a challenge because it is a variable nonlinear stress-strain state within a sheet that must meet four conditions. Two models have been developed to determine the value of plastic deformation, updated Lagrangian formulation and Eulerian formulation. When processed at low or room temperature, there is a strong hardening effect based on Drucker's postulate for stable plastic materials or the postulate of plastic potential. The generated FEM model for deep drawing follows the temperature field, velocity field and plastic deformations in the wall of the extracted element at the given transitional radius of the punch and the die.*

Key words: *Deep drawing, FEM model, Stress, Strain, Velocity, Temperature*

1. INTRODUCTION

Estimates of the world economy show that, on a global level, about 420 billion different types of metal cans (small or larger containers) are produced annually for the needs of food packaging and other consumer goods, with a continuous tendency to increase. Out of that number, 330 billion units refer to unavoidable beverage cans, most often made of an aluminum alloy, while about 85 billion units refer to other metal packaging, both for food and non-food products. Of the total price per unit of such

***Received: Jun 22, 2022 / Accepted Avgust 29, 2022.**
Corresponding author: Saša Ranđelović
Full professor, Aleksandra Medvedeva 14, 18000 Niš
E-mail: sassa@masfak.ni.ac.rs

© 2022 by Faculty of Mechanical Engineering, University of Niš, Serbia

packaged food products, 50% to 70% refers to the metal packaging itself. These numbers indicate that this is a mass-producing industry where profits are very high and where small technological solutions and improvements can greatly reduce variable costs (reducing sheet metal thickness by 0.1mm brings incredible savings).

Fig. 1 Metal containers as packaging

Sheet metal forming is the most common metal shaping process used in the history [1]. Most anisotropic yield functions have been based on the associated flow rule hypothesis. This approach is based on the normality hypothesis that describes the equality of the plastic potential function (which determines the flow direction) and the yield function (which determines the transition from the elastic to the plastic regime). Several studies have evaluated the accuracy of the associated flow-rule based yield functions for the description of various levels of anisotropy. For instance, Yoon et al. [2] reported that the quadratic Hill (1948) and non-quadratic Yld2000-2d [3] yield functions can only predict 4 ears for a deep drawn cup made of an aluminium alloy AA2090-T3 which exhibits 6 ears in experiments. The authors [6] reported similar limitations for the same material based on the anisotropic yield function [7]. Therefore, it can be concluded that it is difficult to describe a highly anisotropic material by means of a model in which an identical formulation for the yield function and plastic potential function is used [8].

Sheet metals exhibit either isotropic or anisotropic yielding behavior. An isotropic yield surface is assigned to a material with identical mechanical properties at different orientations. Various isotropic yield functions are available such as von Mises, Tresca, Hosford, Hershey, Barlat and Richmond, Bishop, Hill, Bassani, Budianski. However, sheet metals are prone to anisotropic behavior which is mainly related to the rolling direction [9]. This is because sheet metals (generally) undergo severe plastic deformations during manufacturing processes such as cold rolling. This introduces preferential orientations to the grains. Consequently, the material obtains a direction dependent mechanical behavior. Material anisotropy highly affects the distribution of stresses and strains and consequently the shape of the final parts, their thickness and possible instabilities such as wrinkling for a deep drawn part.

2. Theoretical basis

Besides the measure of plastic deformation and the plastic stress-strain relations, we need four more data points for the analysis of plastic deformation. These four things are as follows [4].

The first is that, in metal forming processes, the metal first behaves elastically for small deformation and then behaves plastically as the deformation grows. Therefore, we need a criterion which tells us when the elastic behavior ends and the plastic behavior begins. Such a criterion is called the yield criterion. It is usually represented as a scalar function of the stress components. We need to develop the (initial) yield criterion of the metal used. Second, for achieving continued or subsequent plastic deformation beyond initial yielding, additional stress needs to be applied. It means, in subsequent yielding, the initial yield criterion keeps changing with the level of plastic deformation. This phenomenon is called hardening. To model the hardening behavior, we need to develop the criterion for subsequent yielding. Third, when a combination of the stress components decreases, the material again behaves elastically. This is called the unloading phenomenon. To model this phenomenon, we need to develop the unloading criterion. Fourth, the constitutive equation for plastic behavior is usually expressed either in the rate form or in the increment form [5]. The stress tensors which appear in these constitutive equations have to be objective, i.e., they have to be invariant under a change of reference frame. Whereas the Cauchy stress tensor is objective, its rate or increment is not objective.

Therefore, we need to develop the objective stress rate and objective incremental stress measures. A constitutive equation for large elastic deformation is also sometimes expressed in the rate or incremental form. In that case, the stress measures appearing in these constitutive equations also have to be objective.

Two common measures of plastic deformation, namely the incremental linear strain tensor and the strain rate tensor, are developed. The first is valid only for a small incremental deformation and the relation between the two measures is also discussed. The incremental linear strain tensor is useful in the analysis of processes such as forging, deep drawing, and sheet bending, etc., which are amenable to incremental formulation, called the updated Lagrangian formulation [4, 5].

We have noted that a gradient of a vector is a tensor. Therefore, the quantity $\nabla(\boldsymbol{du})$, which is a gradient of the vector $\boldsymbol{du}$ with respect to the current position vector $\boldsymbol{x}$, is a tensor. Since the gradient is not in line with the initial configuration, here the operator ∇ does not have the subscript zero as in the gradient symbol. The components of $\nabla(\boldsymbol{du})$ with respect to the (x, y, z) coordinate system are given by:

$$\nabla(du)=\begin{bmatrix} \frac{\partial(du_x)}{\partial x} & \frac{\partial(du_x)}{\partial y} & \frac{\partial(du_x)}{\partial z} \\ \frac{\partial(du_y)}{\partial x} & \frac{\partial(du_y)}{\partial y} & \frac{\partial(du_y)}{\partial z} \\ \frac{\partial(du_z)}{\partial x} & \frac{\partial(du_z)}{\partial y} & \frac{\partial(du_z)}{\partial z} \end{bmatrix} \tag{1}$$

We have seen that if $\boldsymbol{u}$ is the displacement from the initial configuration to a deformed configuration, then the symmetric part of the gradient of $\boldsymbol{u}$ (with respect to the position vector in the initial configuration) can be chosen as a measure of that deformation, provided the deformation is small. Now, assume that the incremental deformation from the current configuration is small. Mathematically, this assumption means that the components of the tensor $\nabla(\boldsymbol{du})$ are small compared to 1. Since $\boldsymbol{du}$ is the incremental displacement from the current configuration, the symmetric part of the tensor $\nabla(\boldsymbol{du})$ can be selected as a measure of the incremental deformation. Thus, our measure of incremental deformation is tensor $\boldsymbol{d\varepsilon}$, which is the symmetric part of $\nabla(\boldsymbol{du})$ called the incremental linear strain tensor [4, 5].

The relation between tensor $\boldsymbol{d\varepsilon}$ and incremental deformation $\boldsymbol{du}$, in tensor notation, as

$$d\varepsilon = \frac{1}{2}\left[\nabla(du) + (\nabla(du)^T)\right] \tag{2}$$

is called the incremental strain-displacement relations.

To find the incremental displacements, incremental strains and incremental stresses in a deformable body, one needs to solve three sets of incremental equations in the current configuration. Such a formulation is called the updated Lagrangian formulation. The above equation is a first set of governing equations for this formulation when the incremental deformation is small [1].

The physical interpretation of the components of $\boldsymbol{d\varepsilon}$ is similar to that of the components of the linear strain tensor. The component $d\varepsilon_{xx}$ represents the change in current length per unit of the current length along the *x*-direction. The components $d\varepsilon_{yy}$ and $d\varepsilon_{zz}$ have a similar interpretation. The component $d\varepsilon_{xy}$ represents half the change in angle between the directions which are currently along *x* and *y* directions. The components $d\varepsilon_{yz}$ and $d\varepsilon_{zx}$ have a similar interpretation. The sign convention for the components of $\boldsymbol{d\varepsilon}$ is the same as that of the components of the linear strain tensor. Just like the linear strain tensor, the tensor $\boldsymbol{d\varepsilon}$ has principal values, principal directions, principal invariants and the hydrostatic and deviatoric parts. They are defined similarly. The incremental volumetric strain $d\varepsilon_v$, when the incremental deformation is small, is defined by the equation:

$$d\varepsilon_v = d\varepsilon_{ii} \tag{3}$$

It can be shown that, the tensor $\boldsymbol{d\omega}$ represents the incremental rotation of a neighborhood of the particle at time d*t*:

$$d\omega = \frac{1}{2}\left[\nabla(du) - (\nabla(du)^T)\right] \tag{4}$$

The rotation is small if the components of the tensor $\nabla(\boldsymbol{du})$ are small compared to 1. It is called the incremental infinitesimal rotation tensor.

The strain rate tensor is employed in the analysis of rolling, drawing, extrusion, etc., where the analysis is carried out by fixing a region in space (called the control volume) and observing the deformation of the material particles as they pass through the control volume. This formulation is known as the Eulerian formulation.

In this formulation, it is not convenient to analyze the deformation increment by increment. Instead, it is easier to study the deformation of the whole control volume simultaneously. This becomes possible by choosing the velocity as a primary variable (instead of the incremental displacement). Further, in this case, it is the rate of deformation which is the more relevant secondary variable than the deformation itself [4].

3. FEM MODELING OF THE DEEP DRAWING PROCESS

A cylindrical deep drawing element was chosen for the analysis, and as it is an axisymmetric stress-strain state, it is enough to take one-eighth of the entire blank in order to make the process modeling more efficient (Fig. 2). The preparation has a radius $\boldsymbol{R_0}$ = 33mm and a thickness $\boldsymbol{s}$ = 1.5mm, the radius of the punch is $\boldsymbol{R_i}$ = 14mm with a radius $\boldsymbol{r_i}$ = 7mm. The radius of the moving matrix is $\boldsymbol{R_m}$ = 16mm with a transition radius $\boldsymbol{r_m}$ = 6mm. The constructive clearance between the die and the punch is 2mm.

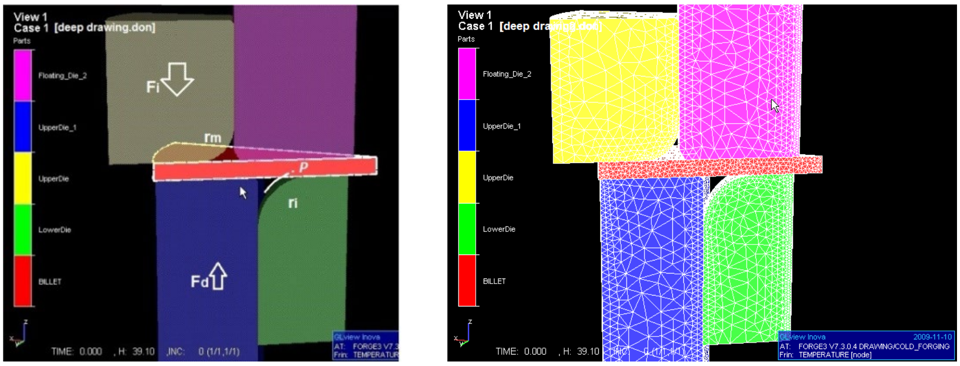

Fig. 2 3D model of deep drawing tool and FEM mesh of the key parts

The final height of the deep drawing part is $\boldsymbol{h_i}$ = 37.4mm. The density of the sheet metal is ρ = 2700 kg/m^3, Young's modulus $\boldsymbol{E}$ = 206·10^6 N/mm^2, Poisson's ratio ν = 0.3 and yield stress σ_o = 235 N/mm^2 are known for the blank material (Fig. 3).

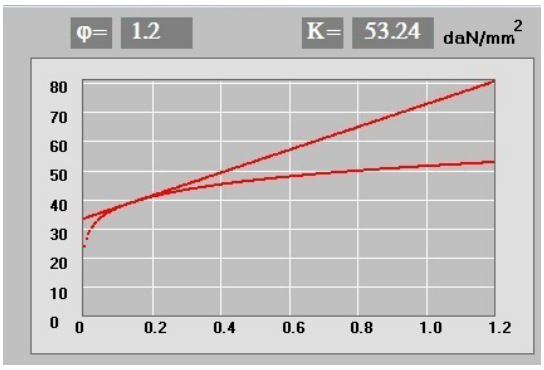

Fig. 3 True stress vs. true strain curve of aluminum alloy

On the FEM 3D model, we have several characteristic contact surfaces on which the coefficients of friction are defined, which have a decisive influence on the deep drawing process. The coefficient of friction between the blank and the flat surfaces of the die, i.e., at the transition radius $\boldsymbol{r_m}$, is $\boldsymbol{\mu_p}$ = 0.15. The coefficient of friction between the blank and the sheet blank holder is $\boldsymbol{\mu_b}$ = 0.1, while the coefficient of friction between the punch and the blank is not taken into account here because the relative movement and sliding of the blank around the surface of the punch almost does not exist.

Each of the tool elements can be represented by a FEM spatial network that can only follow the elastic deformations of key tool elements in order to approach their optimization of the shape, geometry and dimensions of key parameters.

To get the rate of deformation based on the FEM analysis, a small piece of blank volume (the so-called control volume) has been traced during the deep drawing process (Fig. 2). Point *P* indicates the location of a particle in the material. The typical trajectory of the material particle is also shown in Figure 2. Let $\boldsymbol{x}$ be the position vector of point *P* and $\boldsymbol{v}$ be its velocity:

$$v = v_x \hat{i} + v_y \hat{j} + v_z \hat{k} \tag{5}$$

We define the tensor $\nabla \boldsymbol{v}$ (at point *P*) as the gradient of $\boldsymbol{v}$ with respect to the position vector $\boldsymbol{x}$. It is called the velocity gradient tensor. Its components with respect to the (*x, y, z*) coordinate system are given by:

$$\nabla v = \begin{bmatrix} \frac{\partial v_x}{\partial x} & \frac{\partial v_x}{\partial y} & \frac{\partial v_x}{\partial z} \\ \frac{\partial v_y}{\partial x} & \frac{\partial v_y}{\partial y} & \frac{\partial v_y}{\partial z} \\ \frac{\partial v_z}{\partial x} & \frac{\partial v_z}{\partial y} & \frac{\partial v_z}{\partial z} \end{bmatrix} \tag{6}$$

We decompose the tensor $\nabla \boldsymbol{v}$ into a sum of symmetric and antisymmetric parts. Let us define the tensor $\dot{\boldsymbol{\varepsilon}}$ as the symmetric part of $\nabla \boldsymbol{v}$:

$$\dot{\varepsilon} = \frac{1}{2}\left[\nabla v + (\nabla v)^T\right] \tag{7}$$

It can be shown that the tensor $\dot{\boldsymbol{\varepsilon}}$ completely describes the rate of deformation at a point. That is, given the tensor $\dot{\boldsymbol{\varepsilon}}$ at point *P*, we can find the rate of change of length per unit length in any direction at that point. Further, we can also find the rate of change of angle between any pair of perpendicular directions at that point [2, 3, 5]. The tensor $\dot{\boldsymbol{\varepsilon}}$ is called the strain rate tensor. The tensor $\dot{\boldsymbol{\varepsilon}}$ represents the rate of deformation at a point irrespective of whether the rate of deformation at that point is small or large. Further, even though we use the symbol $\dot{\boldsymbol{\varepsilon}}$, commonly employed in metal forming literature for this tensor, it is to be noted that this tensor is not the time derivative of the linear strain tensor $\boldsymbol{\varepsilon}$. In references to continuum mechanics, this tensor is usually denoted by $\boldsymbol{D}$ and is called the rate of deformation tensor [7].

Hardening behavior is modeled by developing a criterion for subsequent yielding. While doing so, it is assumed that the hardening is isotropic. The first approach for developing the plastic stress-strain relations is based on Drucker's postulate for stable plastic material. The second approach is based on the postulate of plastic potential. Starting from the postulate of plastic potential, we firstly discuss the associated flow rule and then develop the following two constitutive equations:

- elastic-plastic incremental stress-strain relation for the updated Lagrangian formulation and
- elastic-plastic stress-strain rate relations for the Eulerian formulation.

While developing these relations, it is assumed that the elastic and plastic parts of the deformation are additive. This is true for the incremental linear strain tensor only when the incremental deformation is small. For the strain rate tensor, it is true if the rotation is small.

The movable die (yellow color), in the upper part of the tool, with its action through the increasing drawing force $\boldsymbol{F_i}$ (Fig. 2), acts on the round blank (red color) which is in continuous contact with all moving and fixed parts of the tool. Fixed adhesion at the bottom of the drawing element (magenta color) ensures controlled plastic deformation and the necessary ejection of the finished part at the end of the deep drawing process from the die. On the moving die, the transitional radius of the die $\boldsymbol{r_m}$ plays an important role over which the deep drawing process takes place. This radius can be given if the geometry of the finished part with the flange is defined or constructively chosen if the finished part without the flange is being drawn out, where it is necessary to draw out the whole part through the die. A necessary tool element for this type of plastic deformation is almost always a blank holder (blue color) which provides (protects?) the entire process of deep drawing (Fig. 2) from the unwanted appearance of wrinkles on the flange of the element. Its pressure on the annular part of the blank, over the force $\boldsymbol{F_d}$ should be constant with the fact that the surface under the blank holder is constantly decreasing during the deep drawing process. With the blank holder, we ensure the nonappearance of wrinkles on the flange of the element, i.e., the normal stress in the radial direction is increased so that the normal stress in the tangential direction would not cause the appearance of wrinkles. The high force of the blank holder can increase the normal stresses in the radial direction largely, so in the case of thinner blanks it is very easy to break the structure of the part and cracks may appear near the transition radius.

This paper aims to present a multi-criteria h-adaptation approach based on error estimators and mesh metrics intersections, which has been successfully introduced in the FORGE® software. It allows one to automatically and dynamically generate meshes adapted to very complex flows and geometries with a very high parallel efficiency.

Fully parallel meshing and remeshing is performed using the so-called topological mesher combined with partitioning/repartitioning strategies [5, 6]. This mesher enables one to generate an anisotropic mesh (2354 tetrahedral elements) by using a linear tensorial field as an input called the mesh metric. This metric is obtained through the combination of three metric fields. The first metric is deduced from an error estimator dedicated to the adaptation of the mesh to the material flow and physical data variations capture. The second metric, skin metric, is deduced from a skin adaptation strategy, and the third is a metric based on geometrical curvature adaptation.

The increase of stress in the radial direction occurs due to plastic deformation of the sheet metal (75%), due to friction on the contact surfaces of the die, blank and blank holder (15%) and due to bending and straightening on rounded tool edges (5%).

The process of metal forming by the technology of deep drawing follows the increase of the temperature inside the metal continuum in the moving focus of deformation. Namely, the change of shape and a large degree of deformation near the transition radius causes an increase in temperature from the reference 20°C to the level of 32.57°C near the radius of the punch. As the deep drawing process takes place, so does the temperature peak near the node 1950 of 23.75°C move over the sheet volume (Fig. 4). If the deformations are larger, i.e., if the deep extraction takes place over a smaller radius, then the irreversible heat generation is more pronounced. In this simulation model, the temperature peak shifts as the deep drawing process takes place. At the end of the interval, the deformed metal continuum reaches a temperature of 47.24°C, but at a transition radius with a die, where the frictional force at the contact of the tool and the blank material also contributes to that (Fig. 4).

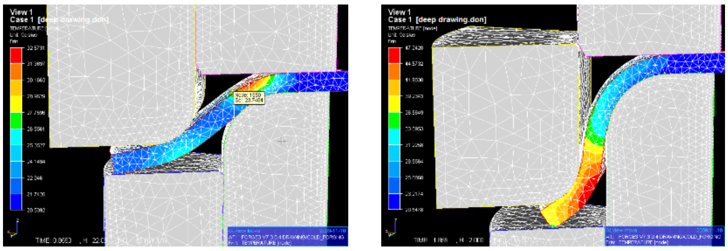

Fig. 4 The temperature field near the transfer radius, node 1950

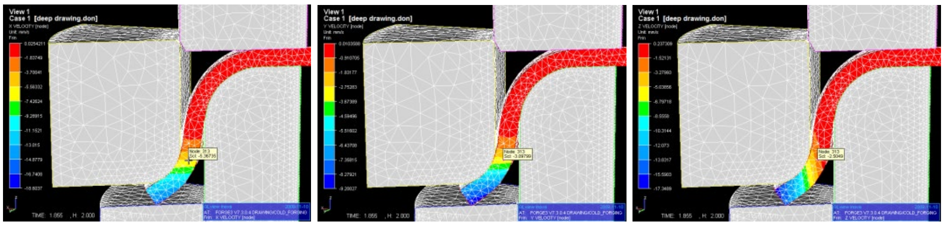

Fig. 5 Velocity field in the *x*, *y* and *z* directions near the transfer radius of the die (node 313)

As a consequence of plastic deformation, there is an intense movement of the material parts, which is manifested by different speeds of the selected node in the directions of the *x*, *y* and *z* coordinate axes (Fig. 5). The selected node of the finite element network 313 has the following velocity v_x = 5.36mm/s, v_y = 3.09mm/s and v_z = 2.05mm/s.

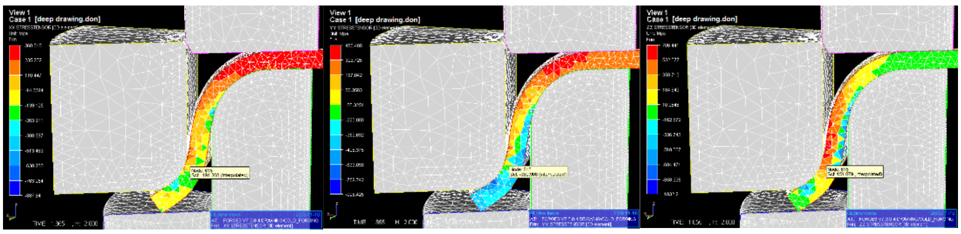

Fig. 6 Elements of stress tensor σ_{xx}, σ_{yy} and σ_{zz} near the transfer radius of the die (node 615)

The field of plastic deformations corresponds to the field of principal stresses that can be followed by the volume of deformed sheet metal (Fig. 6). The principal stresses of the tensor in the selected node 615 at the transition radius of the moving die have the following values: σ_{xx} = -191.25 N/mm^2, σ_{yy} = -380.9 N/mm^2, σ_{zz} = 151.08 N/mm^2. As this is the end of the deep drawing process, negative stresses in the tangential direction and positive stresses in the radial direction dominate, which can often cause destruction of the drawing element because the force of the blank holder is not proportional to the contact surface, i.e., higher pressures than the optimal have occurred. This does not include the variability and optimal values of the force of the blank holder because it requires a special analysis of the deep drawing technology.

The stress distribution in the domain of plasticity, according to Von Mises, is given in Fig. 7, where the critical element is precisely the radius of the die at the final moment of deep drawing. The software recognizes the occurrence of unwanted wrinkles that appear on the walls of the real drawing element.

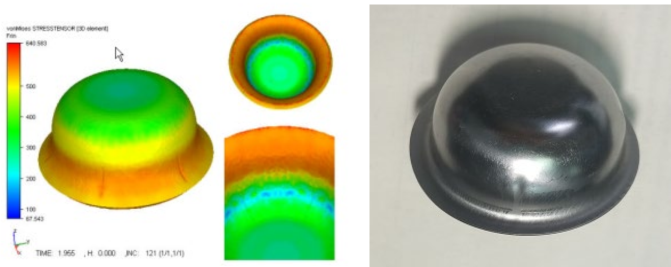

Fig. 7 The Von Mises stress disposition on the wall of the deep-drawn element

4. Conclusion

The FEM model presented in the paper just about perfectly reflects the state of the material in terms of the temperature field and stress field according to the wrinkle of the deep-drawn element. The temperature field according to the wall thickness shows good values of temperature in the nodes of the finite element mesh with the measured values on the wall. In the areas with intense plastic deformation, we have a larger increase in temperature, while at the bottom, where there is no change in shape, that part of the volume remains at the level of the external (ambient) temperature. The relative velocities in the *x* and *y* directions have almost the same change over the height of the part, while the change in the *z* direction is somewhat different because in that direction we have an increase in the height of the part.

Acknowledgement: *This research was financially supported by the Ministry of Education, Science and Technological Development of the Republic of Serbia (Contract No. 451-03-68/2022-14/ 200109*

REFERENCES

1. Marciniak, Z., Duncan, J.L., Hu, S.J., 2002, Mechanics of Sheet Metal Forming, Butterworth-Heinemann.
2. Yoon, J.W., Stoughton, T.B., Dick, R.E., 2007, Earing prediction in cup drawing based on non-associated flow rule, in: CeasarDeSa, J.M.A., Santos, A.D. (Eds.), NUMIFORM '07: Materials Processing and Design: Modeling, Simulation and Applications, Pts I and II. Amer Inst Physics, Melville, pp. 685-690.
3. Barlat, F., Brem, J.C., Yoon, J.W., Chung, K., Dick, R.E., Lege, D.J., Pourgoghrat, F., Choi, S.H., Chu, E., 2003, Plane stress yield function for aluminum alloy sheets – part 1: theory. International Journal of Plasticity 19, pp. 1297-1319.
4. Hill, R., 1948, A Theory of the Yielding and Plastic Flow of Anisotropic Metals, Proceedings of the Royal Society of London. Series A. Mathematical and Physical Sciences 193, pp.281-297.
5. Souza Neto EA, Perić Dj., Owen DRJ., 2008, Computational Methods for Plasticity, Theory and Application, WILEY, 816 p.
6. Cvitanic, V., Vlak, F., Lozina, Z., 2008, A finite element formulation based on nonassociated plasticity for sheet metal forming, International Journal of Plasticity 24, pp. 646-687.
7. Karafillis, A.P., Boyce, M.C., 1993, A general anisotropic yield criterion using bounds and a transformation weighting tensor, J. Mech. Phys. Solids 41, pp. 1859-1886.
8. Stoughton, T.B., Yoon, J.W., 2009, Anisotropic hardening and non-associated flow in proportional loading of sheet metals, International Journal of Plasticity 25, pp. 1777-1817.
9. Safaei M., 2013, Constitutive Modelling of Anisotropic Sheet Metals Based on a Non-Associated Flow Rule, Faculty of Engineering and Architecture, Ghent University, Belgium